

1 **Bioconcentration and metabolic effects of emerging PFOS alternatives in**  
2 **developing zebrafish**

3  
4 Wenqing Tu<sup>a</sup>, Rubén Martínez<sup>b,c</sup>, Laia Navarro-Martin<sup>b</sup>, Daniel J. Kostyniuk<sup>d</sup>, Christine Hum<sup>d</sup>,  
5 Jing Huang<sup>a</sup>, Mi Deng<sup>a</sup>, Yuanxiang Jin<sup>c</sup>, Hing Man Chan<sup>d</sup>, Jan A. Mennigen<sup>d,\*</sup>

6  
7  
8 <sup>a</sup> *Research Institute of Poyang Lake, Jiangxi Academy of Sciences, Nanchang 330012, China.*

9 <sup>b</sup> *Department of Environmental Chemistry, Institute of Environmental Assessment and Water*  
10 *Research, IDAEA-CSIC, Jordi Girona, Barcelona, Spain.*

11 <sup>c</sup> *Department of Cellular Biology, Physiology and Immunology, Universitat de Barcelona (UB),*  
12 *Barcelona, Spain.*

13 <sup>d</sup> *Department of Biology, University of Ottawa, Ottawa, Ontario, Canada.*

14 <sup>e</sup> *College of Biotechnology and Bioengineering, Zhejiang University of Technology, Hangzhou,*  
15 *310032, China*

16  
17 **Corresponding Author**

18 Dr. Jan A. Mennigen

19 E-mail address: [jan.mennigen@uottawa.ca](mailto:jan.mennigen@uottawa.ca)

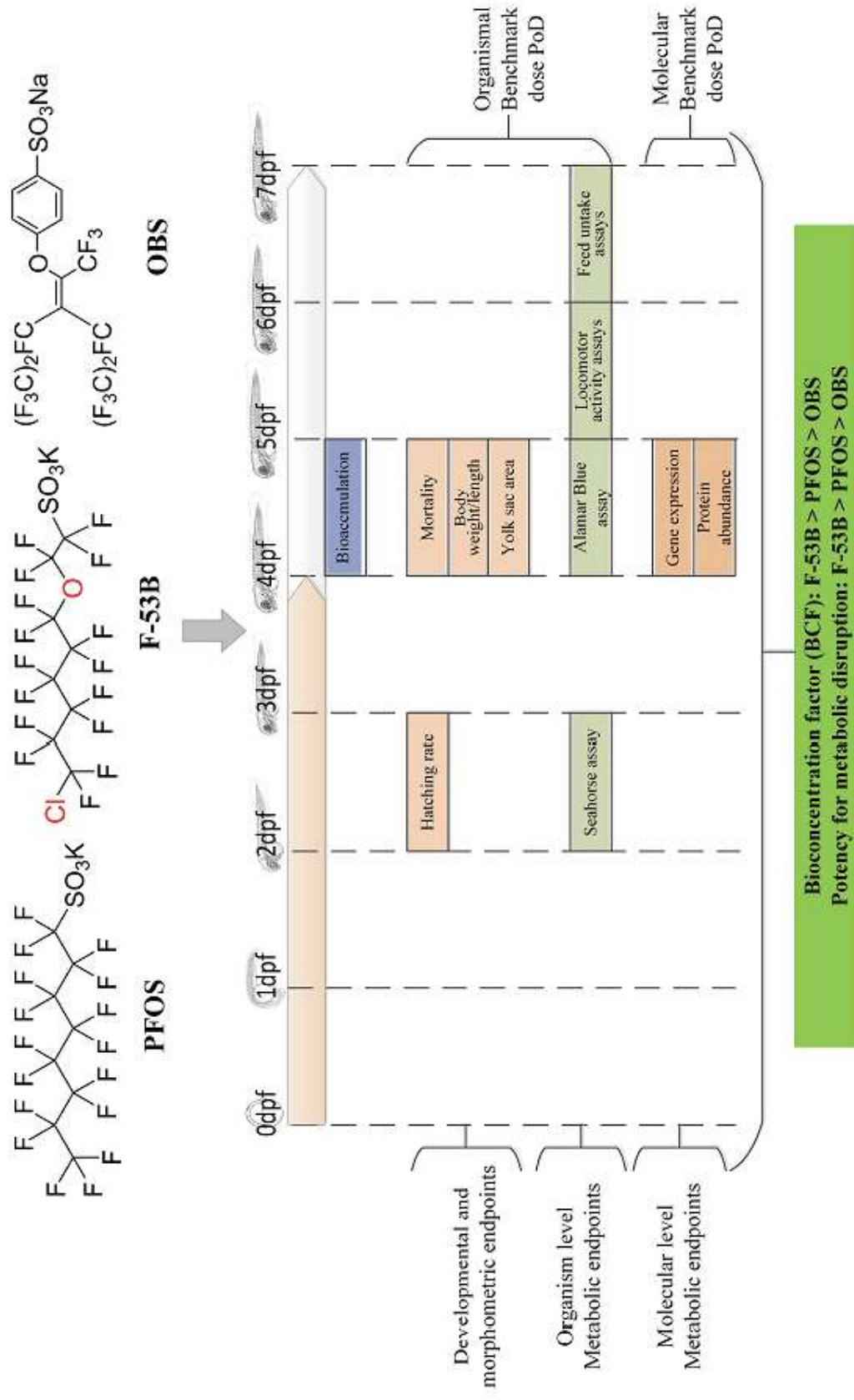
20

## 21 **Abstract**

22 The novel PFOS alternatives 6:2 chlorinated polyfluorinated ether sulfonate (F-53B) and sodium  
23 *p*-perfluorooctanesulfonate (OBS) are emerging in the Chinese market, but little is  
24 known about their ecological risks. In this study, zebrafish embryos were exposed to PFOS, F-  
25 53B and OBS to evaluate their bioconcentration and acute metabolic consequences. Per- and  
26 polyfluoroalkyl substances (PFASs) accumulated in larvae in the order of F-53B > PFOS > OBS,  
27 with the bioconcentration factors ranging from 20 to 357. Exposure to F-53B and PFOS, but not  
28 OBS, increased energy expenditure, and reduced feed intake in a concentration-dependent  
29 manner and the expression of genes involved in metabolic pathways at the transcriptional and  
30 translational levels. Molecular docking revealed that the binding affinities of PFASs to  
31 glucokinase were decreased in the following order: F-53B > PFOS > OBS. Finally, the results of  
32 Point of Departure (PoD) indicate that metabolic endpoints at the molecular and organismal level  
33 are most sensitive to F-53B followed by PFOS and OBS. Collectively, F-53B has the highest  
34 bioconcentration potential and the strongest metabolism-disrupting effects, followed by PFOS  
35 and OBS. Our findings have important implications for the assessment of early developmental  
36 metabolic effects of PFOS alternatives F-53B and OBS in wildlife and humans.

37 **Keywords:** PFOS alternatives; bioconcentration; metabolic disruption; zebrafish; energy balance

## 38 TOC art



39

40

## 41 **1. Introduction**

42 In recent years, 6:2 chlorinated polyfluorinated ether sulfonate (F-53B) and sodium *p*-  
43 perfluorous nonenoxybenzene sulfonate (OBS) have emerged as novel substitutes for  
44 perfluorooctanesulfonic acid (PFOS) in the Chinese market (**Figure S1**). F-53B, which is  
45 structurally similar to PFOS, is used as a chrome mist suppressant in Chinese electroplating  
46 industry, with an annual production of 20-30 tons,<sup>1</sup> while OBS is used in fire-fighting foams and  
47 photographic materials, with an annual production capacity of 3500 tons.<sup>2</sup> Without the same  
48 regulations and restrictions as PFOS on their use, F-53B has been identified in industrial  
49 wastewater, river water and municipal sewage sludge at concentrations ranging from 43 µg/L to  
50 112 µg/L, 2.0 ng/L to 7.6 µg/L and 0.02 ng/g to 209 ng/g, respectively.<sup>3-6</sup> Furthermore, the  
51 accumulation of F-53B was reported in the blood of crucian carp (20.9-41.9 ng/g), marine  
52 mammals (0.023-0.27 ng/g) and human serum (0.8-2.3 ng/mL).<sup>1, 7, 8</sup> In 2017, Xu et al.<sup>9</sup> first  
53 reported the detection of OBS in lake water with a concentration up to 3.2 µg/L. With the  
54 continued use of F-53B and OBS, it is critical to investigate the toxic effects of these  
55 alternatives.

56 In comparison to PFOS, few studies have been conducted to evaluate the bioconcentration  
57 and negative effects of F-53B and OBS. Previous studies have shown that F-53B could  
58 accumulate in aquatic organisms and induce developmental and reproductive toxicity as well as  
59 thyroid endocrine disruption.<sup>10-13</sup> Recently, gut barrier dysfunction and hepatic metabolism  
60 disorder have been found in mice after exposure to OBS.<sup>14</sup> Increasing evidences suggest that  
61 exposure to PFOS has been linked to metabolic disruption. For example, PFOS has been  
62 associated with reduced feed intake and increased spontaneous activity in rodents,<sup>15-18</sup> and a  
63 negative correlation between PFOS exposure and birth weight,<sup>19, 20</sup> and a positive correlation

64 between PFOS exposure and circulating cholesterol and type II diabetes in humans have been  
65 reported.<sup>21,22</sup> In addition, adult zebrafish exposure to PFOS has been also reported to reduce  
66 body weight,<sup>23</sup> induce spontaneous hyperactivity<sup>24-26</sup> and disturb lipid and lipoprotein  
67 metabolism.<sup>27-29</sup> In contrast to these comparatively well-characterized metabolism-disrupting  
68 effects of PFOS, the potential metabolic disrupting potential of the emerging PFOS alternatives  
69 F-53B and OBS is currently unknown.

70 Zebrafish has become an increasingly popular model to study human metabolic diseases  
71 since it possesses conserved metabolic pathways at the genetic level and high homology of  
72 pathways involved in metabolic regulation including energy intake, storage and usage.<sup>30</sup> In this  
73 study, the bioconcentration, developmental toxicity, morphometric endpoints, energy balance at  
74 the levels of feed intake, oxidative energy expenditure and locomotion of F-53B, OBS and PFOS  
75 were studied in early developing zebrafish. To probe metabolic effects at the molecular level, the  
76 key transcripts and proteins involved in the regulation of feed intake and energy expenditure,  
77 glucose and lipid metabolism and somatic growth were quantified. Additionally, molecular  
78 docking was used to further explore the interactions between glucokinase and per- and  
79 polyfluoroalkyl substances (PFASs). Finally, in order to compare metabolic disruption thresholds  
80 at the organismal and transcript level in developing zebrafish, we used endpoints in a benchmark  
81 dose approach to determine the point of Departure (PoD).<sup>31</sup>

## 82 **2. Materials and methods**

### 83 *2.1 Chemicals and reagents*

84 PFOS (purity  $\geq$  98%), F-53B (purity  $\geq$  98%) and OBS (purity  $\geq$  98%) were purchased from  
85 Sigma-Aldrich (Oakville, ON, Canada), Shanghai Maikun Chemical Co., Ltd. (Shanghai, China)  
86 and Ningbo Yongshen Trading Co., Ltd. (Zhejiang, China), respectively. <sup>13</sup>C<sub>4</sub>-labeled <sub>L</sub>-PFOS

87 was obtained from Wellington Laboratories Inc. (Guelph, ON, Canada). All other chemicals and  
88 solvents were of HPLC grade or analytical grade.

## 89 ***2.2 Animal exposure***

90 Wild-type adult zebrafish (AB strain), housed at the University of Ottawa Aquatic Care  
91 Facility, were bred in 1L breeding tanks separated with dividers. Fertilized zebrafish embryos (3  
92 h post-fertilization, hpf) were randomly exposed to various concentrations of PFOS (0.025, 0.25  
93 and 2.5 mg/L), F-53B (0.015, 0.15 and 1.5 mg/L) and OBS (0.04, 0.4 and 4 mg/L). The three  
94 exposure concentrations of each compound were chosen based on 0.1%, 1% and 10% of the  
95 previously established 96 h-LC<sub>50</sub> of each respective compound (unpublished results of W. Tu).  
96 Each treatment and the control (only contained system water; pH 7.5 ± 0.5, conductivity 500 ±  
97 50 µS) were performed in triplicate. Zebrafish embryos/larvae were maintained at 28.5 °C with a  
98 12-h light/12-h dark cycle. All exposure solutions were renewed daily until 4 dpf, after which the  
99 larvae were raised in clean system water. The exposure solutions were sampled at the beginning  
100 of exposure (T<sub>0</sub>) and before the first renewal (T<sub>24</sub>) to measure the actual concentrations of PFASs  
101 in exposure solutions. A rapid decrease in the concentration of PFASs was observed at T<sub>0</sub>, which  
102 was mainly attributed to their adsorption on the surface of glass beakers,<sup>10</sup> while a small  
103 fluctuation was measured at T<sub>24</sub> (**Table S1**). All experimental protocols were approved by the  
104 University of Ottawa's Animal Care and Veterinary Service (ACVS) protocol for the use of  
105 animals in research and teaching (BL-3006).

## 106 ***2.3 Quantification of PFASs in exposure solutions and zebrafish larvae***

107 The extraction of PFASs from the exposure solutions and zebrafish larvae were carried out  
108 in accordance with our previously established protocol for F-53B.<sup>13</sup> Chromatographic separation  
109 was performed on an Eclipse Plus C18 column (1.8 µm × 2.1 mm × 50 mm, Agilent, CA, USA).

110 The mobile phase was 10 mM aqueous ammonium acetate (A) and methanol (B). The solvent  
111 gradient started at 40% B to 100% B over 3 min and was held for 1 min, followed by equilibrium  
112 at 40% B for 1 min. The identification and quantification were carried out on an Agilent 1290  
113 Infinity HPLC System consisting of an Agilent 6420 Triple Quadrupole (Santa Clara, CA, USA)  
114 in the negative ESI mode with multiple reaction monitoring (MRM). Additional details are given  
115 in the Supporting Information ([Text S1](#)).

#### 116 ***2.4 Developmental toxicity and morphometric endpoints***

117 The number of dead embryos/larvae was determined daily. The hatching rate at 48 hpf was  
118 calculated by dividing the number of hatched larvae by the total number of exposed larvae. After  
119 4 days of exposure, 18 larvae from each treatment were randomly selected for body length and  
120 yolk sac area measurement. The yolk sac region contains the entire visible contour surrounding  
121 the yolk sac and the yolk sac extension. Three pools of 60 larvae from each treatment were used  
122 to measure body weight.

#### 123 ***2.5 Energy expenditure assays***

##### 124 ***2.5.1 Seahorse assay***

125 At 2 dpf, zebrafish larvae (n = 15 larvae/treatment) were placed in 500  $\mu$ L system water in  
126 24-well Seahorse islet capture plates as previously described.<sup>32</sup> Following 1 h of acclimation,  
127 plates were run in a Seahorse XF24 machine (Agilent, USA) using the standard energy  
128 phenotype protocol to obtain baseline and stressor-induced oxygen consumption rate (OCR) and  
129 extracellular acidification rate (ECAR). The injected stressor mix (FCCP + oligomycin,  
130 Agilent, CA, USA) resulted in a final well concentration of 3  $\mu$ M FCCP and 8  $\mu$ M oligomycin,  
131 respectively. Data were obtained by repeated measurements at baseline and following the  
132 injection of the stressor mix using the standard Seahorse Agilent energy phenotype kit protocol.

133 Metabolic potential of OCR and ECAR were expressed as ratios between stressor induced and  
134 baseline values for each parameter obtained from the standard Seahorse Agilent energy  
135 phenotype kit protocol.

#### 136 *2.5.2 Alamar Blue assay*

137 Alamar Blue assay, which is dependent on a NADH-, NADPH-, FADH<sub>2</sub>- and FMNH<sub>2</sub>-  
138 based reduction of Alamar Blue (resazurin), has been described as proxy to quantify zebrafish  
139 oxidative metabolism.<sup>33-35</sup> At 4 dpf, zebrafish larvae (n = 72 larvae/treatment) were transferred  
140 into black 96-well plates. This assay was adapted according to the protocol developed by  
141 Renquist et al.<sup>33</sup> The fluorescence at 0 h and 24 h was measured in a fluorescence reader  
142 (Molecular Devices, USA) with excitation and emission wavelengths of 530 nm and 590 nm,  
143 respectively.

#### 144 *2.5.3 Locomotor behavior assay*

145 At 5 dpf, zebrafish larvae (n = 36 larvae/treatment) were transferred into 48-well plates.  
146 Each well contained one larva and 500 µL of system water. The swimming behavior and average  
147 locomotor activity of zebrafish larvae were quantified using the ZebraBox (Viewpoint Behavior  
148 Technology, France). The movement was recorded for a 20-minute period under light condition.  
149 The ViewPoint software (ViewPoint Behavior Technology, France) was used to record the  
150 distance of the movement.

#### 151 *2.6 Feeding assay*

152 At 6 dpf, zebrafish larvae (n = 36 larvae/treatment) were over-fed with commercial  
153 zebrafish food labeled with fluorescent 4-(4-(didecylamino)styryl)-N-methylpyridinium iodide  
154 (4-Di-10-ASP, Sigma-Aldrich, Canada) in Petri dishes. After one hour of feeding, the larvae



155 were collected, washed and homogenized with 300  $\mu$ L of double-distilled water. The 250  $\mu$ L  
156 homogenate was then transferred to a black 96-well plate. The fluorescence was determined by a  
157 fluorescence reader (Molecular Devices, USA) with excitation and emission wavelengths of 485  
158 nm and 535 nm, respectively.

### 159 ***2.7 Targeted metabolic gene expression analysis***

160 At 4 dpf, zebrafish larvae (n = 45 larvae/treatment) were harvested and the total RNA  
161 extraction, first-strand cDNA synthesis and real-time RT-PCR were performed according to the  
162 protocol previously described.<sup>10</sup> The primer sequences for mRNA real-time RT-PCR are shown  
163 in **Table S2**. Prior to the analysis, we carried out a trial and confirmed the stability of  *$\beta$ -actin*  
164 under our experimental conditions. Thus, the housekeeping gene  *$\beta$ -actin* was used as reference  
165 gene for normalization.

### 166 ***2.8 Targeted tissue-specific miRNA analysis***

167 Total RNA was used to synthesize cDNA with HiFlex buffer using the miScript II RT kit  
168 (Qiagen, Toronto, ON, Canada) and Specific miRNAs were subsequently quantified using the  
169 miScript SYBR Green PCR kit (Qiagen, Toronto, ON, Canada) with miRNA-specific forward  
170 primers and a universal reverse primer (**Table S3**). Relative transcript abundance was  
171 normalized to *U6* transcript abundance. More details are provided in the Supporting Information  
172 (**Text S2**)

### 173 ***2.9 Protein extraction and Western blot analysis***

174 The total protein was extracted from zebrafish larvae (4 dpf, n = 45 larvae/treatment)  
175 according to our previously described procedure.<sup>10</sup> Approximately 50  $\mu$ g protein was separated  
176 by SDS-PAGE, then transferred to a polyvinylidene difluoride (PVDF) membrane and probed  
177 with rabbit antibodies raised against neuropeptide Y (NPY; Cell Signaling Technologies,

178 Beverly, MA) or glucokinase (GK; Abcam, Cambridge, UK). Protein levels were quantified by  
179 densitometry analysis, with the results normalized to GAPDH abundance.

### 180 *2.10 Molecular docking analysis*

181 The difference in toxicity of a compound may be attributable to the difference in binding  
182 affinity to the target protein.<sup>36</sup> In this study, since we identified a consistent and strong decrease  
183 in *gk* gene expression in response to all PFASs tested and the important role of GK in the  
184 metabolism of glucose and lipid energy metabolism, GK was selected for molecular docking to  
185 investigate the interactions of PFASs with GK at the atomic level. The 3D structure of zebrafish  
186 glucokinase (zfGK) was built by homology modeling strategy (PDB ID 3FR0) using Modeller  
187 9.14.<sup>37</sup> The quality of the zfGK was evaluated by PROCHECK, ERRAT and Verify 3D in  
188 SAVES (<http://servicesn.mbi.ucla.edu/SAVES/>) and the results indicated that modeled zfGK was  
189 a good quality model (Figure S2). The docked active site of zfGK was defined as the location of  
190 the ligand of the template protein. PFASs were docked into the active site of zfGK using  
191 AutoDock Vina.<sup>38</sup> AutoDock Tools 1.5.6 package (<http://mgltools.scripps.edu>) was employed for  
192 the generation of docking input files and identify the grid center. The superior pose with the  
193 lowest docked energy was selected and visually analyzed by Discovery Studio Visualizer 4.5  
194 (San Diego, CA, USA). More details are provided in the Supporting Information ([Text S3](#)).

### 195 *2.11 Statistical analysis*

196 All individual endpoint data are reported as the mean  $\pm$  standard error of the mean (SEM).  
197 A One-way analysis of variance (ANOVA) followed by Dunnett's post hoc test was conducted to  
198 assess statistical differences between the treatment groups and the control. For Seahorse data, a  
199 two-way ANOVA was used for analysis of treatment groups and stress mix, and their interaction.

200 Statistical significance was determined with a cut-off of  $p < 0.05$ . Data analysis and graphs were  
201 performed using GraphPad Prism version 7.0 (GraphPad, Inc., San Diego, CA, USA).

### 202 ***2.12 Bench mark dose modelling and PoD determination***

203 The benchmark dose (BMD) and Point of Departure (PoD) approaches were utilized to  
204 integrate organismal and molecular endpoints into a comparable endpoint for environmental risk  
205 assessment of metabolic disruption of the PFASs in zebrafish. Briefly, BMDEExpress version 2.2  
206 software (<https://www.sciome.com/bmdexpress/>) was used for the benchmark dose  
207 calculations.<sup>39-41</sup> The best BMD value for each compound and parameter was chosen by the  
208 BMDEExpress software between those established by a third order polynomial, a third order  
209 exponential and a Hill equation, depending on the best-fitted model for each endpoint (**Table**  
210 **S4**).

## 211 **3. Results**

### 212 ***3.1 Bioconcentration of PFASs in developing zebrafish***

213 The concentrations of PFASs in zebrafish larvae showed clear dose-dependent manners  
214 (**Figure 1A**), with 1.4, 24.3 and 160.7 mg/kg wet weight (ww) for PFOS, 1.0, 27.1 and 137.3  
215 mg/kg for F-53B, and 0.6, 14.4 and 114.7 mg/kg for OBS. The calculated bioconcentration  
216 factors (BCFs) were 113-193 for PFOS, 125-358 for F-53B and 20-48 for OBS (**Figure 1B**).

### 217 ***3.2 Zebrafish developmental toxicity and morphometric endpoints are minimally affected by*** 218 ***PFASs***

219 Exposure to PFASs did not significantly affect hatching rate and mortality (**Figure S3**).  
220 However, the yolk sac area was significantly reduced in high F-53B exposure group compared to  
221 the control (**Figure S4A**). PFASs exposure did not significantly affect larval body weight and  
222 body length (**Figure S4B-C**).

### 223 ***3.3 PFASs induce energy balance parameter changes in developing zebrafish***

224 Several aspects of the organismal level metabolic phenotype were significantly affected by  
225 PFASs exposure in early developing zebrafish. Embryo oxygen consumption rate (OCR) was  
226 significantly reduced in high PFOS exposure group (**Figure 2A**) and all OBS exposure groups  
227 irrespective of concentration (**Figure 2C**) compared to the control. The application of the  
228 stressor mix significantly increased OCR in PFASs ( $p < 0.001$ ), while no significant interaction  
229 between treatment and stressor was found (**Figure 2A-C**). This lack of interaction is also evident  
230 in the observed lack of significant effects of OCR potential (**Figure 2D-F**), calculated as the  $\Delta$   
231 between stressor-induced and baseline OCR. Only PFOS significantly increased the extracellular  
232 acidification rate (ECAR) at the low concentration compared to the control (**Figure 2G**). While  
233 exposure to the stressor mix significantly increased ECAR in PFASs ( $p < 0.01$ ), no interaction  
234 effects between PFASs exposure and stressor (**Figure 2G-I**), and no effects on ECAR potential  
235 (**Figure 2J-L**), calculated as the  $\Delta$  between stressor-induced and baseline ECAR, were  
236 identified.

237 Indirect measurement of oxidative energy expenditure using the 24 h Alamar Blue assay  
238 increased significantly in zebrafish exposed to medium and high PFOS concentrations and all F-  
239 53B concentrations (**Figure 3A**). Locomotory behavior, assessed as total distance travelled, was  
240 not significantly affected by exposure to PFASs at any concentration (**Figure 3B**). Feed intake  
241 was significantly reduced in medium and high PFOS exposure groups and all F-53B exposure  
242 groups (**Figure 3C**).

### 243 ***3.4 PFASs differentially affect metabolic gene expression profiles in developing zebrafish***

244 The expression of several transcripts involved in central regulation of energy expenditure  
245 was profiled (**Figure 4A-F**). Compared to the control, *npv* transcript abundance was significantly

246 reduced by high PFOS, low and high F-53B, and medium and high OBS exposure. The *pomca*  
247 transcripts were significantly reduced in larvae exposed to high PFOS and all OBS  
248 concentrations compared to the control. Transcript abundance of *cart* was significantly reduced  
249 in medium OBS exposed larvae compared to the control. No changes in transcript abundance  
250 were observed for *agrp*, *cart2* and *mc4r*. The expression of transcripts involved in glucose  
251 metabolism (**Figure 4G-J**) revealed a significant reduction on *gk* expression in all exposed  
252 zebrafish compared to the control. Transcript abundance of *pck1*, *insa*, and *insb* did not change  
253 significantly in larvae exposed to PFASs. The expression of transcripts involved in lipid  
254 metabolism (**Figure 4K-M**) revealed that PFASs significantly reduced *cpt1a* transcript  
255 abundance in low and high PFOS and F-53B exposure groups and in all OBS exposure groups  
256 compared to the control. No significant differences in transcript abundance of *fasn* and *ppara*  
257 were identified. Both profiled transcripts involved in the hypothalamus-pituitary-somatotropic  
258 (HPS) axis, *gh* and *igf2*, were significantly affected by exposure to PFASs (**Figure 4N-O**).  
259 Transcript abundance of *gh* was significantly reduced by high F-53B and medium OBS  
260 exposure. Transcript abundance of *igf2* was significantly reduced by medium OBS exposure.  
261 Finally, PFASs exposure did not affect the transcriptomic expression of *ucp2* (**Figure 4P**).

### 262 ***3.5 PFASs differentially affect tissue-specific miRNA expression profiles in developing*** 263 ***zebrafish***

264 The expression of several tissue-specific and enriched miRNA transcripts was profiled  
265 (**Figure S5**). Significant changes in response to PFASs exposures were identified for muscle-  
266 specific *miRNA-1* (**Figure S5A**), but not muscle-specific *miRNA-133* (**Figure S5B**), liver-  
267 specific *miRNA-122* (**Figure S5C**) or pancreas-enriched *miRNA-375* (**Figure S5D**). Compared to

268 the control, *miRNA-1* transcript abundance (**Figure S5A**) was significantly reduced by high OBS  
269 exposure.

### 270 **3.6 PFASs exposure reduce GK and NPY protein levels in developing zebrafish**

271 Exposure to PFASs resulted in a dose-dependent decrease in GK protein abundance, but a  
272 significant reduction was observed only in medium and high OBS exposure groups compared to  
273 the control (**Figure 5A-C**). NPY protein abundance (**Figure 5D-F**) was significantly reduced by  
274 high PFOS exposure compared to the control (**Figure 5D**)

### 275 **3.7 Binding potential of PFASs toward zebrafish GK (zfGK)**

276 As illustrated in **Figure 6**, PFASs were docked into the active site of zfGK. The binding  
277 energy and hydrogen bond interactions obtained from docking analysis are listed in **Table S5**. In  
278 the docked complexes, hydrogen bonds were formed between PFOS and residues of Asn70,  
279 Ser138, Thr215 and Gly431; F-53B and residues of Thr155, Asn191, Gly216 and Cys217; and  
280 OBS and residues of Gly68, Thr69, Gly216 and Ser432. The binding affinity of PFASs toward  
281 zfGK in the order of F-53B > PFOS > OBS, and the corresponding binding energies were -7.8, -  
282 6.8 and -6.2 kcal/mol, respectively.

### 283 **3.8 Transcriptomic and organismal PoD of metabolic disruption**

284 The transcriptomic point of departure (PoD) was calculated to be 0.0038, 0.0080 and  
285 0.00141 mg/L for F-53B, PFOS and OBS, respectively (**Figure 7A**). Regarding the PoD for the  
286 organismal level endpoints, the order of PoD thresholds from most sensitive to least sensitive  
287 was maintained albeit at higher thresholds of 0.0063, 0.0122 and 0.9412 mg/L for F-53B, PFOS  
288 and OBS, respectively (**Figure 7B**). A summary of the median BMD and BMDL values for  
289 PFASs can be found in **Table S6**.

## 290 **4. Discussion**

#### 291 ***4.1 Differential accumulation of PFASs in developing zebrafish***

292 The high body burden of PFOS, F-53B and OBS in zebrafish larvae indicates their  
293 bioconcentration potential as other PFASs. The accumulation of PFOS and F-53B has been  
294 previously reported in fish and mammals,<sup>1,7,13</sup> and OBS has been recently found to accumulate in  
295 the liver and gut of mice (unpublished results of W. Tu). To compare the bioconcentration potential  
296 of the three PFASs in developing zebrafish, their respective BCFs were determined. The results  
297 showed that the BCFs of PFOS and F-53B are of the same order of magnitude, which are one  
298 order of magnitude higher than OBS. This suggests chemical structure-specific differences in  
299 uptake, bioconcentration and metabolism. In the terms of medium exposure concentration, F-53B  
300 exhibited twice the bioconcentration potential than PFOS. This is not surprising since F-53B has  
301 been reported to be the most bio-persistent PFASs to date,<sup>42</sup> and the BCF of F-53B was also  
302 found to be significantly higher than that of PFOS in wild crucian carp.<sup>1</sup>

#### 303 ***4.2 PFASs differentially affect organism level metabolic endpoints***

304 Exposure to PFASs did not significantly affect developmental and morphometric  
305 parameters, except for a significant reduction in yolk sac area observed in high F-53B exposure  
306 group. Control group mortality did not exceed 5%, respecting OECD Test 212 guideline  
307 stipulations for fish embryo testing.<sup>43</sup> In contrast, several metabolic endpoints were differentially  
308 affected by PFASs exposures at the organismal level. Reductions in oxygen consumption were  
309 observed in pre-hatching zebrafish embryos at 2 dpf exposed to high PFOS, and all OBS  
310 exposure groups. These results suggest a compound and dose-specific reduction in standard  
311 metabolic rate, with the strongest and most consistent effects in OBS. Extracellular acidification,  
312 a measure of glycolytic flux, was only significantly increased by low PFOS exposure. Together  
313 this data suggests a reduction in energy expenditure, especially in OBS-exposed larvae. Both

314 PFOS and F-53B, but not OBS, concentration-dependently increased 24 h oxidative energy  
315 expenditure and decreased feed intake in post-hatching larvae at 4 dpf, suggesting similar modes  
316 of action of these structurally similar compounds on larval energy balance. While the 24 h  
317 Alamar Blue assay has been described as proxy to quantify zebrafish oxidative metabolism,<sup>33-35</sup> it  
318 is, however, important to acknowledge that locomotion may contribute to increased oxidative  
319 energy expenditure quantified by this assay. While not significant, we observed a tendency for  
320 increased locomotor activity in all PFOS and F-53B, but not OBS exposed larvae compared to  
321 the control, suggesting that the tendency for increased locomotor activity may have contributed  
322 to increased energy expenditure at this developmental stage. Indeed, developmental and adult  
323 PFOS exposure has been linked to increase spontaneous activity and a hyperactive phenotype in  
324 rodents<sup>17,18</sup> and zebrafish.<sup>24-26</sup> Furthermore, in addition to mitochondrial reductases indicative of  
325 oxidative metabolism, other enzymes, including enzymes involved in cellular detoxification and  
326 oxidative stress responses, may affect the reduction of Alamar Blue.<sup>44</sup> Induction of oxidative  
327 stress in zebrafish larvae has recently been reported for both PFOS and F-53B exposures,<sup>13,45</sup>  
328 raising the possibility that active enzymes in detoxification oxidative stress response may have  
329 contributed to the observed significant increase in energy expenditure in PFOS and F-53B  
330 exposed larvae. The concentration-dependent decrease in larval feed-intake exposed to PFOS  
331 and F53B, but not OBS, is in line with previously reported effects in rodent models, where PFOS  
332 was shown to suppress feed intake by stimulating hypothalamic transcript urocortin 2 (*ucn2*) and  
333 brown adipose tissue *ucp2*.<sup>15,16</sup> While brown adipose tissue does not exist in fish, our study  
334 suggests that F-53B, similarly to PFOS, exhibits early onset anorexic and energy expenditure  
335 promoting effects after hatching, potentially via central mechanisms. Together, our findings  
336 show that structurally similar PFOS and F-53B promote a negative organismal energy balance in



337 post-hatch larvae, an early onset effect that, at least in the highest F-53B exposure group, is  
338 linked to increased yolk sac utilization, and may play a role in previously reported PFOS- and F-  
339 53B-dependent decreases in body weight reported in zebrafish.<sup>10,23</sup>

#### 340 ***4.3 PFASs affect transcript and protein abundance involved in energy metabolism***

341 To investigate potential molecular mechanisms that may underlie the organismal metabolic  
342 phenotype in PFASs-exposed larvae, we profiled transcript abundance of genes involved in the  
343 central regulation of energy expenditure, metabolic pathways implicated in glucose and lipid  
344 metabolism, the HPS axis, and mitochondrial uncoupling. A differential reduction in larval  
345 transcript abundance of the orexigenic factor *npv* and the anorexigenic factors *pomc* and *cart*  
346 were observed in groups exposed to PFASs, suggesting potential molecular level effects on  
347 central mediators of energy balance. A significant decrease of *npv* was observed in response to  
348 all PFASs, albeit at different exposure concentrations. Subsequent Western blot analysis  
349 confirmed that at least in high PFOS exposure group, these transcript changes were translated  
350 into a decrease in NPY protein abundance, suggesting a possible role for NPY in the  
351 significantly reduced feed intake in this group. However, it is important to keep in mind that  
352 while zebrafish *npv* is expressed in brain regions involved in the regulation of feed intake and  
353 energy expenditure, it is widely expressed in other regions.<sup>46</sup> This warrants a cautionary  
354 interpretation, and future *in-situ* hybridization studies will be needed to link these changes  
355 specifically to brain areas involved in feed intake and energy expenditure. Significant reductions  
356 of *pomc* and *cart* transcript abundance were largely found in OBS-exposed zebrafish, raising the  
357 possibility that a reduced anorexigenic transcript abundance may have contributed to the lack of  
358 effect on food intake in OBS exposed larvae. Developmental *pomc* expression is centrally

359 restricted to the anterior pituitary region,<sup>47-49</sup> allowing for a more precise interpretation of *pomc*  
360 gene expression changes in whole larvae compared to *npv*.

361 With regard to key metabolic pathways involved in the metabolism of glucose and lipid  
362 energy metabolism, we identified a consistent and strong decrease in *gk* gene expression in  
363 response to all PFASs tested, irrespective of dose. Consistent with this pattern, a dose-dependent  
364 trend for a decrease in GK protein was observed across all exposure groups. Furthermore,  
365 molecular docking studies showed that PFASs fitted well into the active site of zebrafish GK and  
366 form stable interactions through hydrogen bonding, indicating that PFASs may directly affect  
367 GK protein abundance through protein-ligand interactions. GK is a low-affinity enzyme that  
368 distributes glucose to the cytoplasm by catalyzing the initial step of glycolysis by conversion of  
369 glucose to glucose-6-phosphate under high glucose conditions.<sup>50</sup> It is primarily expressed in  
370 liver, pancreas and glucosensing parts of the brain, and contributes to developmental<sup>51</sup> and adult  
371 systemic glucoregulation by acting in all of these tissues in mammals.<sup>52-54</sup> In zebrafish,  
372 ontogenetic *gk* expression is detected at 4 dpf.<sup>55</sup> However, its functional roles other than  
373 inducibility in response to glucose in adult zebrafish liver<sup>56,57</sup> have not been characterized in this  
374 model. While a trend for a decrease in pancreas-specifically expressed *insa* was observed in  
375 zebrafish larvae exposed to PFASs, this decrease was not significant, suggesting *gk* reduction is  
376 not completely due to pancreatic development effects, which have been reported for PFOS.<sup>58</sup> In  
377 spite of relatively well characterized, temporospatial expression profiles obtained from *in situ*  
378 hybridization studies, differential allometric growth may be a factor in affecting tissue-specific  
379 expression profiles, exemplified by *gk*, which is predominantly expressed in hepatopancreatic  
380 tissue and glucosensing areas of the brain.<sup>52-54</sup> Therefore, we quantified several highly tissue-  
381 specific miRNA markers, including liver-specific *miRNA-122*, pancreas-enriched *miRNA-375*,

382 and muscle-specific *miRNA-1/133* to delineate possible effects on tissue differentiation from the  
383 described ubiquitous downregulation of *gk* gene expression transcripts in zebrafish exposed to  
384 PFASs. Because neither *miRNA-122* nor *miRNA-375* significantly altered the expression levels in  
385 groups exposed to PFASs, it is likely that observed *gk* effects are specific and not mediated by  
386 effects of PFASs on the liver or pancreatic tissue differentiation. Conversely, the OBS-specific  
387 decrease on muscle-specific *miRNA-1*, but not *miRNA-133*, suggests muscle-specific effects of  
388 OBS exposure. Indeed, *miRNA-1* and *miRNA-133* have been shown to play central roles in the  
389 balance of striated muscle proliferation and differentiation.<sup>59, 60</sup> Future work should therefore  
390 explore possible functional consequences of OBS induced downregulation of *miRNA-1*. The  
391 transcript abundance of *pck1*, the rate-limiting enzyme in *de novo* gluconeogenesis, which is  
392 expressed and functions in zebrafish glucoregulation in early development,<sup>61</sup> and in liver and  
393 pronephros of developing zebrafish,<sup>62</sup> did not change significantly across groups exposed to  
394 PFASs. Transcripts related to lipid-metabolism revealed that PFASs affected both rate-limiting  
395 lipogenic (*fasn*) and  $\beta$ -oxidation (*cpt1a*) transcripts, however, only *cpt1a* transcript abundance  
396 revealed significant changes compared to control groups. Together, these transcriptional changes  
397 point to early onset effects of PFASs exposure on rate-limiting glucose and lipid metabolic  
398 pathways. PFASs exposure differentially affected transcript levels of the HPS axis, with a  
399 consistent decrease in both *gh* and *igf2* in zebrafish exposed to medium OBS. This response is  
400 indicative of a concentration- and the compound-specific response of the HPS axis to OBS, at  
401 least at the transcript level. PFASs exposure did not affect transcript levels of *ucp2*, suggesting  
402 that mitochondrial uncoupling, at least at the transcriptional level, was not affected by PFASs  
403 exposure in post-hatch larvae.

404 ***4.4 PoD analysis reveals higher sensitivity for metabolic disruption in developing zebrafish***  
405 ***exposed to F-53B and PFOS compared to OBS***

406 In order to integrate quantified transcript and organismal level endpoints to assess sublethal  
407 metabolic effects of PFASs exposure, we determined separate PoDs using a Benchmark dose  
408 approach for transcriptomic and organism level responses. While transcript PoDs were more  
409 sensitive compared to organismal PoDs, the order of sensitivity from lowest to highest threshold  
410 is maintained at both levels of biological organization (F-53B < PFOS < OBS; **Figure 7A-B**). In  
411 the case of the PFOS (0.0080 and 0.0122 mg/L, respectively) and F-53B (0.0038 and 0.0063  
412 mg/L, respectively), the transcript and organismal level PoDs are in the same order of  
413 magnitude, and relatively similar between both compounds compared to OBS. This observation  
414 points to the fact that metabolic transcript responses to PFOS and F-53B exposure are a good  
415 approximation of organismal metabolic effects, and that F-53B and PFOS have similar PoDs for  
416 sublethal metabolic effects at both levels of organization, likely caused by their similar chemical  
417 structure, which allows them to interact similarly with cellular targets. Interestingly, a recent  
418 transcriptomic level analysis of PFOS at different concentrations resulted in a similar PoD in the  
419 same order of magnitude (0.011 mg/L), whereas the PoD for morphometric parameters was  
420 identified to be 2.53 mg/L.<sup>63</sup> This suggests that while the targeted metabolic subset of transcripts  
421 is reflective of whole transcriptome level PoD for PFOS in developing zebrafish, the organism-  
422 level metabolic phenotype is more susceptible to alteration in response to low concentration  
423 PFOS exposure compared to strictly morphometric endpoints. In case of gene expression and  
424 whole organism parameters, F-53B elicited sublethal metabolic responses at a two-fold lower  
425 threshold compared to PFOS. Taking into account that F-53B is found in the environment at  
426 concentrations comparable to PFOS<sup>3</sup> and the F-53B PoD threshold concentration of metabolic

427 disruption at both the organismal and molecular level is in the range of reported aquatic  
428 environmental F-53B concentrations,<sup>3-5</sup> our study raises concerns over F-53B-induced sublethal  
429 metabolic disruption in early development in wild-life and humans. Clearly, long-term studies in  
430 the zebrafish and other models are warranted to address potential long-term metabolic  
431 consequences, especially given the reported environmental persistence and bioconcentration of  
432 the compound across development and even generations,<sup>10, 12, 13</sup> as well as reported long-term  
433 metabolic consequences of developmental PFASs exposure in manipulative rodent and human  
434 epidemiological studies.<sup>64, 65</sup>

435 On the other hand, OBS presented the lowest PoDs for sublethal metabolic effects of the  
436 three PFASs tested (0.0141 and 0.9412 mg/L for the transcriptomic and organismal level  
437 endpoint, respectively), suggesting that the different chemical structure of this compound affects  
438 transcript and organism-level metabolic responses differently and with lower potency. It is,  
439 however, possible that OBS affects other pathways not related to energy metabolism with higher  
440 potency, and future transcriptome level studies should investigate this possibility.

441 Interestingly, a consistently lower threshold for transcript compared to organismal  
442 metabolic disruption PoD exists in developing zebrafish, suggesting that molecular markers can  
443 be used as a sensitive early indicator that precedes the onset of organismal level metabolic  
444 disruption effects. While the order of sensitivities (F-53B < PFOS < OBS) is maintained at both  
445 levels, the margin between molecular and organism level metabolic disruption PoD is much  
446 higher for OBS (approximately two orders of magnitude) than the differences between the  
447 respective PoDs for F-53B and PFOS (in the same order of magnitude), suggesting a smaller  
448 safety margin between identification of molecular level metabolic effects and organismal level  
449 effects for F-53B and PFOS.

450 In conclusion, our study reveals previously unknown sublethal effects of the Chinese PFOS  
451 replacement compound F-53B on energy metabolism across early development in the zebrafish  
452 model. F-53B exposure affects both metabolic transcript level and organismal metabolic  
453 phenotype at a two-fold lower PoD both at both levels of the biological organization compared to  
454 PFOS, a known metabolic disruptor. Given the widespread use of F-53B as PFOS replacement in  
455 China, this raises concerns about metabolic disruption during early development, and future  
456 studies are warranted to assess potential long-term consequences of the metabolic phenotype  
457 within and across generations. Compared to F-53B, exposure to OBS elicits metabolic disruption  
458 in larvae only at higher concentrations, especially at the organismal level, suggesting a  
459 comparatively lower potency for metabolic disruption in early development. Nevertheless, our  
460 study identified glucokinase transcript abundance as an endpoint potentially disrupted by all  
461 PFASs, and future studies are warranted to validate this transcript as a potential sensitive marker  
462 for developmental PFASs exposure in general.

### 463 **Acknowledgements**

464 This research work was supported by the National Natural Science Foundation of China  
465 (41867064 and 31860154), the Spanish Ministry of Education, Culture and Sport (FPU15/03332  
466 and EST18/00001), the European Commission H2020-Marie Skłodowska-Curie Action MSCA-  
467 IF-RI-2017 (797725 EpiSTOX), and the Natural Sciences and Engineering Research Council of  
468 Canada (147476) and Canada Foundation of Innovation (148035).

### 469 **Supporting Information Available**

470 Additional information including supplemental texts (**Text S1-3**), supplemental tables  
471 (**Table S1-6**) and supplemental figures (**Figure S1-6**). This information is available free of  
472 charge via the internet at <http://pubs.acs.org>.

473 **Disclosures**

474       The authors declare no competing financial interest.

475

476 **References**

- 477 1. Shi, Y.; Vestergren, R.; Zhou, Z.; Song, X.; Xu, L.; Liang, Y.; Cai, Y. Tissue distribution  
478 and whole body burden of the chlorinated polyfluoroalkyl ether sulfonic acid F-53B in crucian  
479 carp (*Carassius carassius*): Evidence for a highly bioaccumulative contaminant of emerging  
480 concern. *Environ. Sci. Technol.* **2015**, *49* (24), 14156-14165.
- 481 2. Bao, Y.; Qu, Y.; Huang, J.; Cagnetta, G.; Yu, G.; Weber, R. First assessment on  
482 degradability of sodium p-perfluorooctane sulfonate (OBS), a high volume  
483 alternative to perfluorooctane sulfonate in fire-fighting foams and oil production agents in China.  
484 *RSC Adv.* **2017**, *7* (74), 46948-46957.
- 485 3. Wang, S.; Huang, J.; Yang, Y.; Hui, Y.; Ge, Y.; Larssen, T.; Yu, G.; Deng, S.; Wang, B.;  
486 Harman, C. First report of a Chinese PFOS alternative overlooked for 30 years: its toxicity,  
487 persistence, and presence in the environment. *Environ. Sci. Technol.* **2013**, *47* (18), 10163-  
488 10170.
- 489 4. Lin, Y.; Liu, R.; Hu, F.; Liu, R.; Ruan, T.; Jiang, G. Simultaneous qualitative and  
490 quantitative analysis of fluoroalkyl sulfonates in riverine water by liquid chromatography  
491 coupled with Orbitrap high resolution mass spectrometry. *J. Chromatogr. A* **2016**, *1435*, 66-74.
- 492 5. Wang, T.; Vestergren, R.; Herzke, D.; Yu, J.; Cousins, I. T. Levels, isomer profiles, and  
493 estimated riverine mass discharges of perfluoroalkyl acids and fluorinated alternatives at the  
494 mouths of Chinese rivers. *Environ. Sci. Technol.* **2016**, *50* (21), 11584-11592.
- 495 6. Ruan, T.; Lin, Y.; Wang, T.; Liu, R.; Jiang, G. Identification of novel polyfluorinated  
496 ether sulfonates as PFOS alternatives in municipal sewage sludge in China. *Environ. Sci.*  
497 *Technol.* **2015**, *49* (11), 6519-6527.
- 498 7. Gebbink, W. A.; Bossi, R.; Rigét, F. F.; Rosing-Asvid, A.; Sonne, C.; Dietz, R.  
499 Observation of emerging per- and polyfluoroalkyl substances (PFASs) in Greenland marine  
500 mammals. *Chemosphere* **2016**, *144*, 2384-2391.
- 501 8. Pan, Y.; Zhu, Y.; Zheng, T.; Cui, Q.; Buka, S. L.; Zhang, B.; Guo, Y.; Xia, W.; Yeung, L.  
502 W.; Li, Y.; Zhou, A.; Qiu, L.; Liu, H.; Jiang, M.; Wu, C.; Xu, S.; Dai, J. Novel chlorinated  
503 polyfluorinated ether sulfonates and legacy per-/polyfluoroalkyl substances: placental transfer  
504 and relationship with serum albumin and glomerular filtration rate. *Environ. Sci. Technol.* **2016**,  
505 *51* (1), 634-644.
- 506 9. Xu, L.; Shi, Y.; Li, C.; Song, X.; Qin, Z.; Cao, D.; Cai, Y. Discovery of a novel  
507 polyfluoroalkyl benzenesulfonic acid around oilfields in northern China. *Environ. Sci. Technol.*  
508 **2017**, *51* (24), 14173-14181.
- 509 10. Deng, M.; Wu, Y.; Xu, C.; Jin, Y.; He, X.; Wan, J.; Yu, X.; Rao, H.; Tu, W. Multiple  
510 approaches to assess the effects of F-53B, a Chinese PFOS alternative, on thyroid endocrine  
511 disruption at environmentally relevant concentrations. *Sci. Total Environ.* **2018**, *624*, 215-224.
- 512 11. Shi, G.; Cui, Q.; Pan, Y.; Sheng, N.; Sun, S.; Guo, Y.; Dai, J. 6:2 Chlorinated  
513 polyfluorinated ether sulfonate, a PFOS alternative, induces embryotoxicity and disrupts cardiac  
514 development in zebrafish embryos. *Aquat. Toxicol.* **2017**, *185*, 67-75.
- 515 12. Shi, G.; Guo, H.; Sheng, N.; Cui, Q.; Pan, Y.; Wang, J.; Guo, Y.; Dai, J. Two-  
516 generational reproductive toxicity assessment of 6:2 chlorinated polyfluorinated ether sulfonate  
517 (F-53B, a novel alternative to perfluorooctane sulfonate) in zebrafish. *Environ. Pollut.* **2018**, *243*,  
518 1517-1527.



- 519 13. Wu, Y.; Deng, M.; Jin, Y.; Liu, X.; Mai, Z.; You, H.; Mu, X.; He, X.; Alharthi, R.;  
520 Kostyniuk, D. J.; Yang, C.; Tu, W. Toxicokinetics and toxic effects of a Chinese PFOS  
521 alternative F-53B in adult zebrafish. *Ecotoxicol. Environ. Saf.* **2019**, *171*, 460-466.
- 522 14. Wang, C.; Zhang, Y.; Deng, M.; Wang, X.; Tu, W.; Fu, Z.; Jin, Y. Bioaccumulation in  
523 the gut and liver causes gut barrier dysfunction and hepatic metabolism disorder in mice after  
524 exposure to low doses of OBS. *Environ. Int.* **2019**, *129*, 279-290.
- 525 15. Asakawa, A.; Toyoshima, M.; Fujimiya, M.; Harada, K.; Ataka, K.; Inoue, K.; Koizumi,  
526 A. Perfluorooctane sulfonate influences feeding behavior and gut motility via the hypothalamus.  
527 *Int. J. Mol. Med.* **2007**, *19* (5), 733-739.
- 528 16. Shabalina, I. G.; Kramarova, T. V.; Mattsson, C. L.; Petrovic, N.; Rahman Qazi, M.;  
529 Csikasz, R. I.; Chang, S. C.; Butenhoff, J.; DePierre, J. W.; Cannon, B.; Nedergaard, J. The  
530 environmental pollutants perfluorooctane sulfonate and perfluorooctanoic acid upregulate  
531 uncoupling protein 1 (UCP1) in brown-fat mitochondria through a UCP1-dependent reduction in  
532 food intake. *Toxicol. Sci.* **2015**, *146* (2), 334-343.
- 533 17. Johansson, N.; Fredriksson, A.; Eriksson, P. Neonatal exposure to perfluorooctane  
534 sulfonate (PFOS) and perfluorooctanoic acid (PFOA) causes neurobehavioural defects in adult  
535 mice. *Neurotoxicology* **2008**, *29* (1), 160-169.
- 536 18. Onishchenko, N.; Fischer, C.; Wan Ibrahim, W. N.; Negri, S.; Spulber, S.; Cottica, D.;  
537 Ceccatelli, S. Prenatal exposure to PFOS or PFOA alters motor function in mice in a sex-related  
538 manner. *Neurotox. Res.* **2011**, *19* (3), 452-461.
- 539 19. Apelberg, B. J.; Witter, F. R.; Herbstman, J. B.; Calafat, A. M.; Halden, R. U.; Needham,  
540 L. L.; Goldman, L. R. Cord serum concentrations of perfluorooctane sulfonate (PFOS) and  
541 perfluorooctanoate (PFOA) in relation to weight and size at birth. *Environ. Health Perspect.*  
542 **2007**, *115* (11), 1670-1676.
- 543 20. Ashley-Martin, J.; Dodds, L.; Arbuckle, T. E.; Bouchard, M. F.; Fisher, M.; Morriset, A.  
544 S.; Monnier, P.; Shapiro, G. D.; Ettinger, A. S.; Dallaire, R.; Taback, S.; Fraser, W.; Platt, R. W.  
545 Maternal concentrations of perfluoroalkyl substances and fetal markers of metabolic function  
546 and birth weight. *Am. J. Epidemiol.* **2017**, *185* (3), 185-193.
- 547 21. Sun, Q.; Zong, G.; Valvi, D.; Nielsen, F.; Coull, B.; Grandjean, P. Plasma concentrations  
548 of perfluoroalkyl substances and risk of type 2 diabetes: a prospective investigation among US  
549 women. *Environ. Health Perspect.* **2018**, *126* (3), 037001.
- 550 22. Nelson, J. W.; Hatch, E. E.; Webster, T. F. Exposure to polyfluoroalkyl chemicals and  
551 cholesterol, body weight, and insulin resistance in the general U.S. population. *Environ. Health*  
552 *Perspect.* **2010**, *118* (2), 197-202.
- 553 23. Wang, M.; Chen, J.; Lin, K.; Chen, Y.; Hu, W.; Tanguay, R. L.; Huang, C.; Dong, Q.  
554 Chronic zebrafish PFOS exposure alters sex ratio and maternal related effects in F1 offspring.  
555 *Environ. Toxicol. Chem.* **2011**, *30* (9), 2073-2080.
- 556 24. Chen, J.; Das, S. R.; La Du, J.; Corvi, M. M.; Bai, C.; Chen, Y.; Liu, X.; Zhu, G.;  
557 Tanguay, R. L.; Dong, Q.; Huang, C. Chronic PFOS exposures induce life stage-specific  
558 behavioral deficits in adult zebrafish and produce malformation and behavioral deficits in F1  
559 offspring. *Environ. Toxicol. Chem.* **2013**, *32* (1), 201-206.
- 560 25. Spulber, S.; Kilian, P.; Wan Ibrahim, W. N.; Onishchenko, N.; Ulhaq, M.; Norrgren, L.;  
561 Negri, S.; Di Tuccio, M.; Ceccatelli, S. PFOS induces behavioral alterations, including  
562 spontaneous hyperactivity that is corrected by dexamfetamine in zebrafish larvae. *PLoS One*  
563 **2014**, *9* (4), e94227.

- 564 26. Jantzen, C. E.; Annunziato, K. M.; Cooper, K. R. Behavioral, morphometric, and gene  
565 expression effects in adult zebrafish (*Danio rerio*) embryonically exposed to PFOA, PFOS, and  
566 PFNA. *Aquat. Toxicol.* **2016**, *180*, 123-130.
- 567 27. Du, Y.; Shi, X.; Liu, C.; Yu, K.; Zhou, B. Chronic effects of water-borne PFOS exposure  
568 on growth, survival and hepatotoxicity in zebrafish: a partial life-cycle test. *Chemosphere* **2009**,  
569 *74* (5), 723-729.
- 570 28. Cheng, J.; Lv, S.; Nie, S.; Liu, J.; Tong, S.; Kang, N.; Xiao, Y.; Dong, Q.; Huang, C.;  
571 Yang, D. Chronic perfluorooctane sulfonate (PFOS) exposure induces hepatic steatosis in  
572 zebrafish. *Aquat. Toxicol.* **2016**, *176*, 45-52.
- 573 29. Cui, Y.; Lv, S.; Liu, J.; Nie, S.; Chen, J.; Dong, Q.; Huang, C.; Yang, D. Chronic  
574 perfluorooctanesulfonic acid exposure disrupts lipid metabolism in zebrafish. *Hum. Exp. Toxicol.*  
575 **2017**, *36* (3), 207-217.
- 576 30. Seth, A.; Stemple, D. L.; Barroso, I. The emerging use of zebrafish to model metabolic  
577 disease. *Dis. Mod. Mech.* **2013**, *6* (5), 1080-1088.
- 578 31. Davis, J. A.; Gift, J. S.; Zhao, Q. J. Introduction to benchmark dose methods and U.S.  
579 EPA's benchmark dose software (BMDS) version 2.1.1. *Toxicol. Appl. Pharmacol.* **2011**, *254*  
580 (2), 181-191.
- 581 32. Stackley, K. D.; Beeson, C. C.; Rahn, J. J.; Chan, S. S. Bioenergetic profiling of zebrafish  
582 embryonic development. *PLoS One* **2011**, *6* (9), e25652.
- 583 33. Renquist, B. J.; Zhang, C.; Williams, S. Y.; Cone, R. D. Development of an assay for  
584 high-throughput energy expenditure monitoring in the zebrafish. *Zebrafish* **2013**, *10* (3), 343-  
585 352.
- 586 34. Williams, S. Y.; Renquist, B. J. High throughput *danio rerio* energy expenditure assay. *J.*  
587 *Vis. Exp.* **2016**, (107), e53297.
- 588 35. Reid, R. M.; D'Aquila, A. L.; Biga, P. R. The validation of a sensitive, non-toxic in vivo  
589 metabolic assay applicable across zebrafish life stages. *Comp. Biochem. Physiol. C Toxicol.*  
590 *Pharmacol.* **2018**, *208*, 29-37.
- 591 36. Lu, L.; Zhan, T.; Ma, M.; Xu, C.; Wang, J.; Zhang, C.; Liu, W.; Zhuang, S. Thyroid  
592 disruption by bisphenol S analogues via thyroid hormone receptor  $\beta$ : in vitro, in vivo, and  
593 molecular dynamics simulation study. *Environ. Sci. Technol.* **2018**, *52* (11), 6617-6625.
- 594 37. Eswar, N.; Webb, B.; Marti-Renom, M. A.; Madhusudhan, M. S.; Eramian, D.; Shen, M.  
595 Y.; Pieper, U.; Sali, A. Comparative protein structure modeling using MODELLER. *Curr.*  
596 *Protoc. Protein Sci.* **2007**, *Chapter 2*, Unit 2 9.
- 597 38. Trott, O.; Olson, A. J. AutoDock Vina: improving the speed and accuracy of docking  
598 with a new scoring function, efficient optimization, and multithreading. *J. Comput. Chem.* **2010**,  
599 *31* (2), 455-461.
- 600 39. Yang, L.; Allen, B. C.; Thomas, R. S. BMDExpress: a software tool for the benchmark  
601 dose analyses of genomic data. *BMC Genomics* **2007**, *8*, 387.
- 602 40. Kuo, B.; Francina Webster, A.; Thomas, R. S.; Yauk, C. L. BMDExpress Data Viewer-a  
603 visualization tool to analyze BMDExpress datasets. *J. Appl. Toxicol.* **2016**, *36* (8), 1048-1059.
- 604 41. Phillips, J. R.; Svoboda, D. L.; Tandon, A.; Patel, S.; Sedykh, A.; Mav, D.; Kuo, B.;  
605 Yauk, C. L.; Yang, L.; Thomas, R. S.; Gift, J. S.; Davis, J. A.; Olszyk, L.; Merrick, B. A.;  
606 Paules, R. S.; Parham, F.; Saddler, T.; Shah, R. R.; Auerbach, S. S. BMDExpress 2: enhanced  
607 transcriptomic dose-response analysis workflow. *Bioinformatics* **2019**, *35* (10), 1780-1782.

- 608 42. Shi, Y.; Vestergren, R.; Xu, L.; Zhou, Z.; Li, C.; Liang, Y.; Cai, Y. Human exposure and  
609 elimination kinetics of chlorinated polyfluoroalkyl ether sulfonic acids (Cl-PFESAs). *Environ.*  
610 *Sci. Technol.* **2016**, *50* (5), 2396-2404.
- 611 43. Horie, Y.; Yamagishi, T.; Takahashi, H.; Shintaku, Y.; Iguchi, T.; Tatarazako, N.  
612 Assessment of the lethal and sublethal effects of 20 environmental chemicals in zebrafish  
613 embryos and larvae by using OECD TG 212. *J. Appl. Toxicol.* **2017**, *37* (10), 1245-1253.
- 614 44. Rampersad, S. N. Multiple applications of Alamar Blue as an indicator of metabolic  
615 function and cellular health in cell viability bioassays. *Sensors (Basel)* **2012**, *12* (9), 12347-  
616 12360.
- 617 45. Sant, K. E.; Sinno, P. P.; Jacobs, H. M.; Timme-Laragy, A. R. Nrf2a modulates the  
618 embryonic antioxidant response to perfluorooctanesulfonic acid (PFOS) in the zebrafish, *Danio*  
619 *rerio*. *Aquat. Toxicol.* **2018**, *198*, 92-102.
- 620 46. Söderberg, C.; Wraith, A.; Ringvall, M.; Yan, Y.-L.; Postlethwait, J. H.; Brodin, L.;  
621 Larhammar, D. Zebrafish genes for neuropeptide Y and peptide YY reveal origin by  
622 chromosome duplication from an ancestral gene linked to the homeobox cluster. *J. Neurochem.*  
623 **2002**, *75* (3), 908-918.
- 624 47. Hansen, I. A.; To, T. T.; Wortmann, S.; Burmester, T.; Winkler, C.; Meyer, S. R.;  
625 Neuner, C.; Fassnacht, M.; Allolio, B. The pro-opiomelanocortin gene of the zebrafish (*Danio*  
626 *rerio*). *Biochem. Biophys. Res. Co.* **2003**, *303* (4), 1121-1128.
- 627 48. Liu, N. A.; Huang, H.; Yang, Z.; Herzog, W.; Hammerschmidt, M.; Lin, S.; Melmed, S.  
628 Pituitary corticotroph ontogeny and regulation in transgenic zebrafish. *Mol. Endocrinol.* **2003**, *17*  
629 (5), 959-966.
- 630 49. Sun, L.; Xu, W.; He, J.; Yin, Z. In vivo alternative assessment of the chemicals that  
631 interfere with anterior pituitary POMC expression and interrenal steroidogenesis in POMC:  
632 EGFP transgenic zebrafish. *Toxicol. Appl. Pharmacol.* **2010**, *248* (3), 217-225.
- 633 50. Lenzen, S. A fresh view of glycolysis and glucokinase regulation: history and current  
634 status. *J. Biol. Chem.* **2014**, *289* (18), 12189-12194.
- 635 51. Hattersley, A. T.; Beards, F.; Ballantyne, E.; Appleton, M.; Harvey, R.; Ellard, S.  
636 Mutations in the glucokinase gene of the fetus result in reduced birth weight. *Nat. Genet.* **1998**,  
637 *19* (3), 268-270.
- 638 52. Hayashi, H.; Sato, Y.; Li, Z.; Yamamura, K.; Yoshizawa, T.; Yamagata, K. Roles of  
639 hepatic glucokinase in intertissue metabolic communication: Examination of novel liver-specific  
640 glucokinase knockout mice. *Biochem. Biophys. Res. Commun.* **2015**, *460* (3), 727-732.
- 641 53. De Backer, I.; Hussain, S. S.; Bloom, S. R.; Gardiner, J. V. Insights into the role of  
642 neuronal glucokinase. *Am. J. Physiol. Endocrinol. Metab.* **2016**, *311* (1), E42-55.
- 643 54. Lu, B.; Kurmi, K.; Munoz-Gomez, M.; Jacobus Ambuludi, E. J.; Tonne, J. M.; Rakshit,  
644 K.; Hitosugi, T.; Kudva, Y. C.; Matveyenko, A. V.; Ikeda, Y. Impaired beta-cell glucokinase as  
645 an underlying mechanism in diet-induced diabetes. *Dis. Model. Mech.* **2018**, *11* (6), 1-12.
- 646 55. Rocha, F.; Dias, J.; Engrola, S.; Gavaia, P.; Geurden, I.; Dinis, M. T.; Panserat, S.  
647 Glucose overload in yolk has little effect on the long-term modulation of carbohydrate metabolic  
648 genes in zebrafish (*Danio rerio*). *J. Exp. Biol.* **2014**, *217* (Pt 7), 1139-1149.
- 649 56. Robison, B. D.; Drew, R. E.; Murdoch, G. K.; Powell, M.; Rodnick, K. J.; Settles, M.;  
650 Stone, D.; Churchill, E.; Hill, R. A.; Pappasani, M. R.; Lewis, S. S.; Hardy, R. W. Sexual  
651 dimorphism in hepatic gene expression and the response to dietary carbohydrate manipulation in  
652 the zebrafish (*Danio rerio*). *Comp. Biochem. Physiol. Part D Genomics Proteomics* **2008**, *3* (2),  
653 141-154.

- 654 57. Gonzalez-Alvarez, R.; Ortega-Cuellar, D.; Hernandez-Mendoza, A.; Moreno-Arriola, E.;  
655 Villasenor-Mendoza, K.; Galvez-Mariscal, A.; Perez-Cruz, M. E.; Morales-Salas, I.; Velazquez-  
656 Arellano, A. The hexokinase gene family in the zebrafish: structure, expression, functional and  
657 phylogenetic analysis. *Comp. Biochem. Physiol. B Biochem. Mol. Biol.* **2009**, *152* (2), 189-195.
- 658 58. Sant, K. E.; Jacobs, H. M.; Borofski, K. A.; Moss, J. B.; Timme-Laragy, A. R.  
659 Embryonic exposures to perfluorooctanesulfonic acid (PFOS) disrupt pancreatic organogenesis  
660 in the zebrafish, *Danio rerio*. *Environ. Pollut.* **2017**, *220* (Pt B), 807-817.
- 661 59. Mishima, Y.; Abreu-Goodger, C.; Staton, A. A.; Stahlhut, C.; Shou, C.; Cheng, C.;  
662 Gerstein, M.; Enright, A. J.; Giraldez, A. J. Zebrafish miR-1 and miR-133 shape muscle gene  
663 expression and regulate sarcomeric actin organization. *Genes Dev.* **2009**, *23* (5), 619-632.
- 664 60. Chen, J.-F.; Mandel, E. M.; Thomson, J. M.; Wu, Q.; Callis, T. E.; Hammond, S. M.;  
665 Conlon, F. L.; Wang, D.-Z. The role of microRNA-1 and microRNA-133 in skeletal muscle  
666 proliferation and differentiation. *Nat. Genet.* **2005**, *38* (2), 228-233.
- 667 61. Jurczyk, A.; Roy, N.; Bajwa, R.; Gut, P.; Lipson, K.; Yang, C.; Covassin, L.; Racki, W.  
668 J.; Rossini, A. A.; Phillips, N.; Stainier, D. Y.; Greiner, D. L.; Brehm, M. A.; Bortell, R.; diIorio,  
669 P. Dynamic glucoregulation and mammalian-like responses to metabolic and developmental  
670 disruption in zebrafish. *Gen. Comp. Endocrinol.* **2011**, *170* (2), 334-345.
- 671 62. Gut, P.; Baeza-Raja, B.; Andersson, O.; Hasenkamp, L.; Hsiao, J.; Hesselson, D.;  
672 Akassoglou, K.; Verdin, E.; Hirsche, M. D.; Stainier, D. Y. Whole-organism screening for  
673 gluconeogenesis identifies activators of fasting metabolism. *Nat. Chem. Biol.* **2013**, *9* (2), 97-  
674 104.
- 675 63. Martinez, R.; Navarro-Martin, L.; Luccarelli, C.; Codina, A. E.; Raldua, D.; Barata, C.;  
676 Tauler, R.; Pina, B. Unravelling the mechanisms of PFOS toxicity by combining morphological  
677 and transcriptomic analyses in zebrafish embryos. *Sci. Total. Environ.* **2019**, *674*, 462-471.
- 678 64. Maisonet, M.; Terrell, M. L.; McGeehin, M. A.; Christensen, K. Y.; Holmes, A.; Calafat,  
679 A. M.; Marcus, M. Maternal concentrations of polyfluoroalkyl compounds during pregnancy and  
680 fetal and postnatal growth in British girls. *Environ. Health. Perspect.* **2012**, *120* (10), 1432-1437.
- 681 65. Wan, H. T.; Zhao, Y. G.; Leung, P. Y.; Wong, C. K. Perinatal exposure to  
682 perfluorooctane sulfonate affects glucose metabolism in adult offspring. *PLoS One* **2014**, *9* (1),  
683 e87137.  
684

685 **Figures captions**

686 **Figure 1.** The concentrations of PFASs (A) and their corresponding bioconcentration factors (B)  
687 in developing zebrafish after 4 days of exposure.

688 **Figure 2.** Effects on oxygen consumption rates (A-C), oxygen consumption rate metabolic  
689 potential (D-F), extracellular acidification rates (G-I) and extracellular acidification-rate  
690 potential (J-L) in 2 dpf zebrafish exposed to various concentrations of PFASs. Asterisks are  
691 indicative of significant differences compared to the control at the  $P < 0.05$  (\*) and  $P < 0.01$  (\*\*)  
692 level, respectively.

693 **Figure 3.** Effects on oxidative metabolism related energy expenditure measured by Alamar Blue  
694 assay in 4 dpf zebrafish (A), locomotor activity assessed as total distance travelled in 20 min in 5  
695 dpf zebrafish (B) and feed intake measured as ingestion of fluorescently labelled food (C) in 6  
696 dpf zebrafish exposed to various concentrations of PFASs. Asterisks are indicative of significant  
697 differences compared to the control at the  $P < 0.05$  (\*) and  $P < 0.01$  (\*\*) level, respectively.

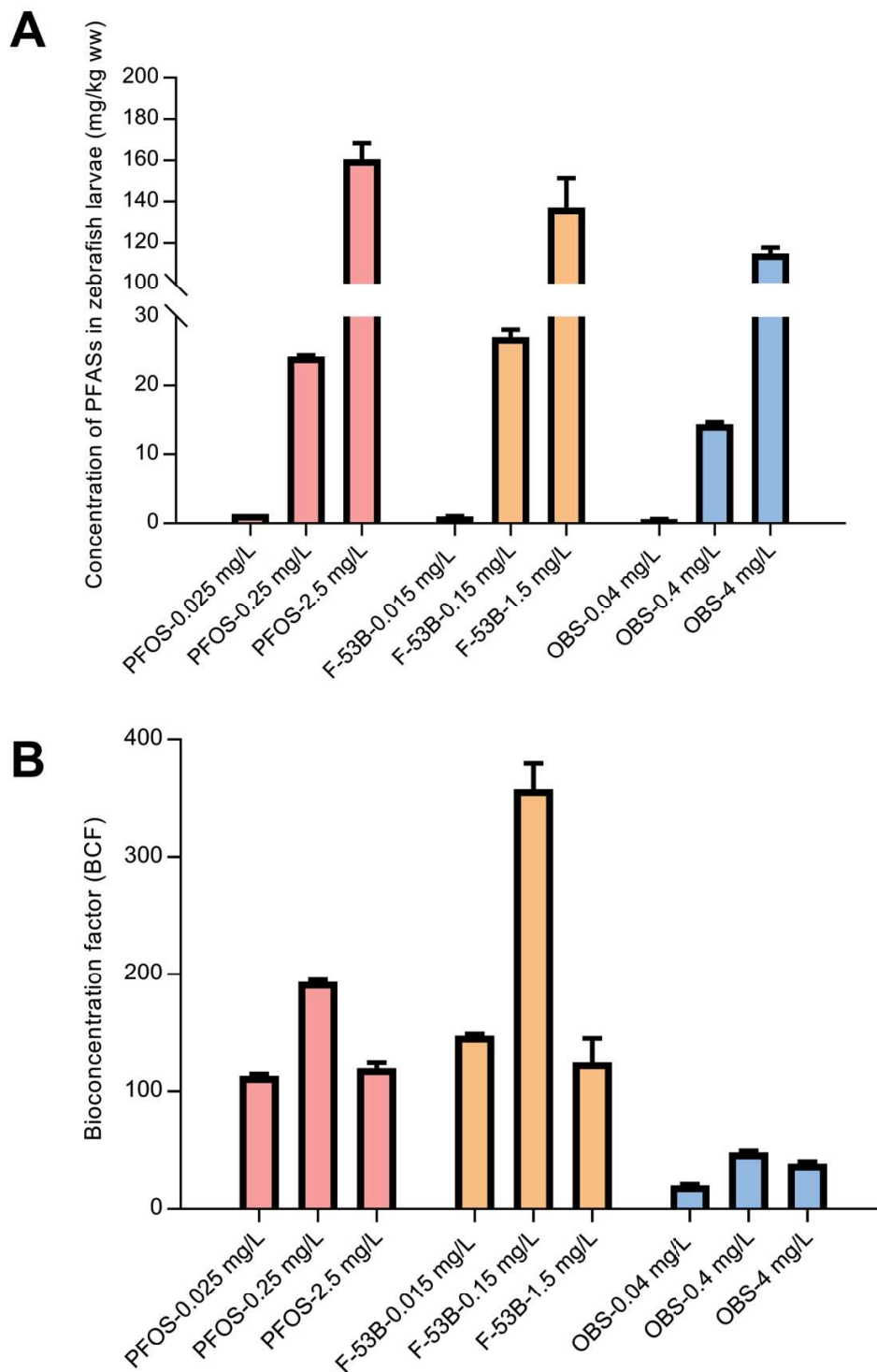
698 **Figure 4.** Effects on abundance of transcripts involved in central regulation of energy  
699 expenditure (A-F), glucose metabolism (G-J), lipid metabolism (K-M), the hypothalamus-  
700 pituitary growth axis (N-O) and mitochondrial uncoupling (P) in 4 dpf zebrafish exposed to  
701 various concentrations of PFASs. Asterisks are indicative of significant differences compared to  
702 the control at the  $P < 0.05$  (\*) and  $P < 0.01$  (\*\*) level, respectively.

703 **Figure 5.** Effects on protein abundance of GK (A-C) and NPY (D-F) in 4 dpf zebrafish exposed  
704 to various concentrations of PFASs. Asterisks are indicative of significant differences compared  
705 to the control at the  $P < 0.05$  (\*) and  $P < 0.01$  (\*\*) level, respectively.

706 **Figure 6.** The active binding site of PFASs toward zebrafish GK (within red ball) (A) and  
707 molecular docking result of PFOS (B), F-53B (C) and OBS (D) with zebrafish GK.

708 **Figure 7.** Accumulation plot of the best calculated BMDs for metabolic transcript- **(A)** and  
709 organism-level endpoints **(B)** The best BMD value for each endpoint was determined by the  
710 BMDEExpress software by identifying the best fitted model for each endpoint between third order  
711 polynomial, third order exponential and a Hill equation models. The median BMDL were used as  
712 PoD (Point of Departure) for each compound and are interpolated in the graph as dotted line  
713 arrows.  
714

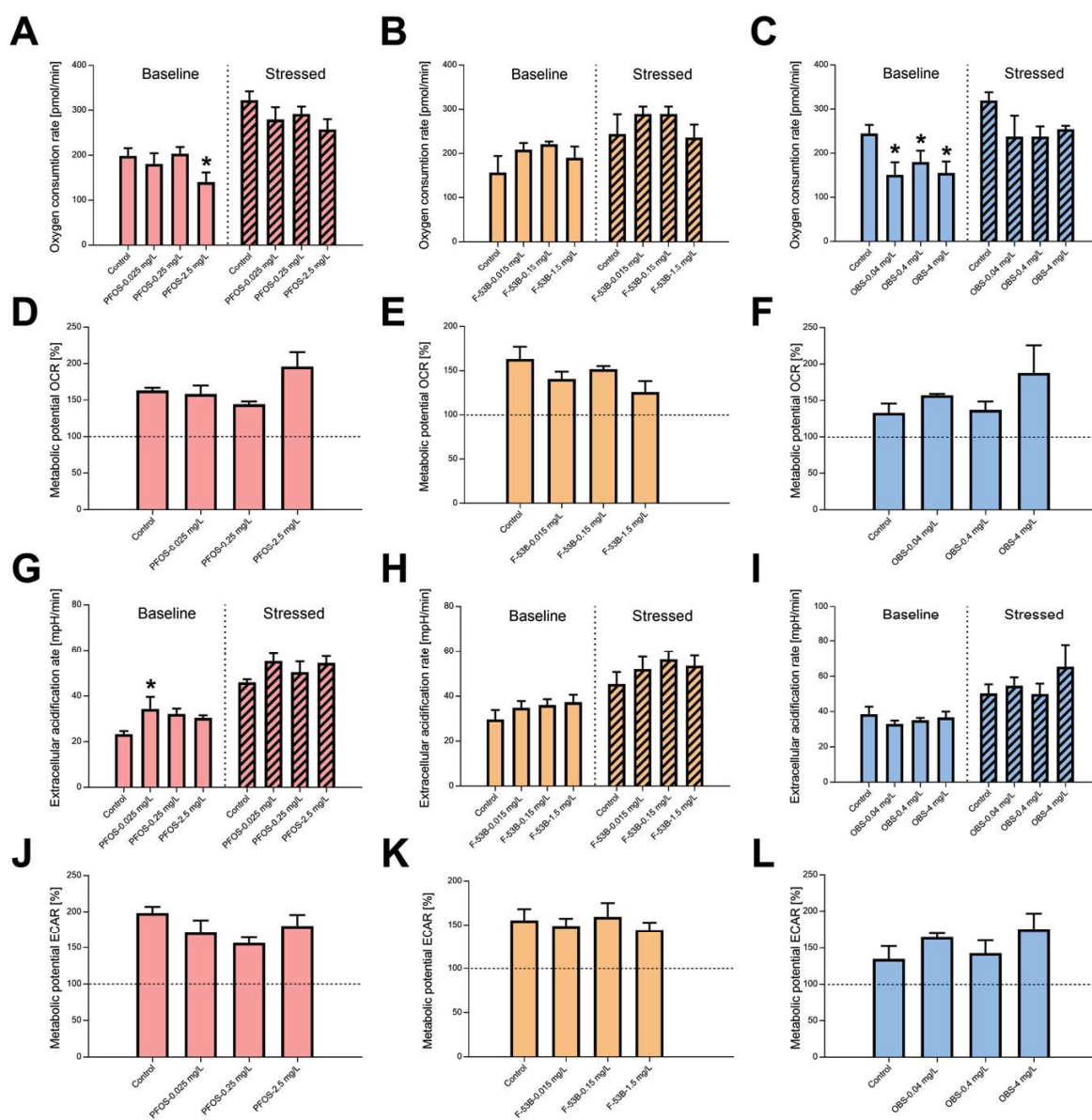
715 **Figure 1**



716

717

718 **Figure 2**

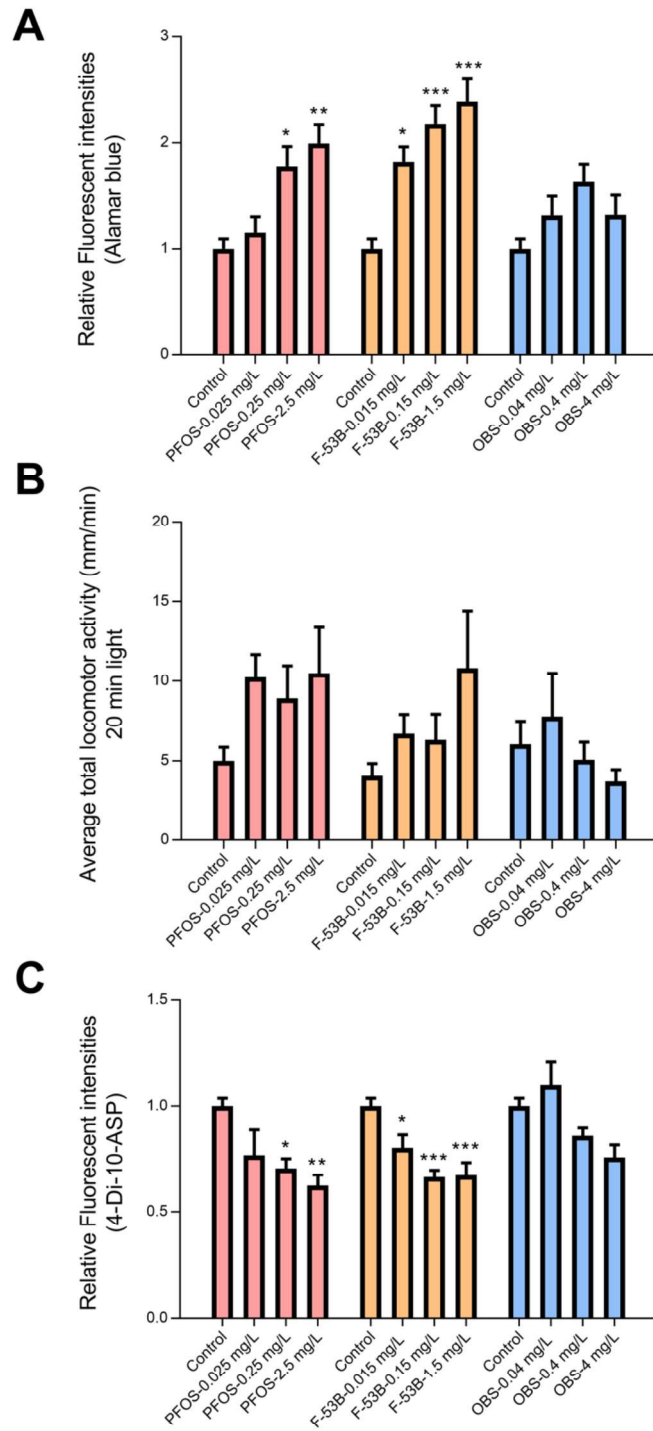


719

720



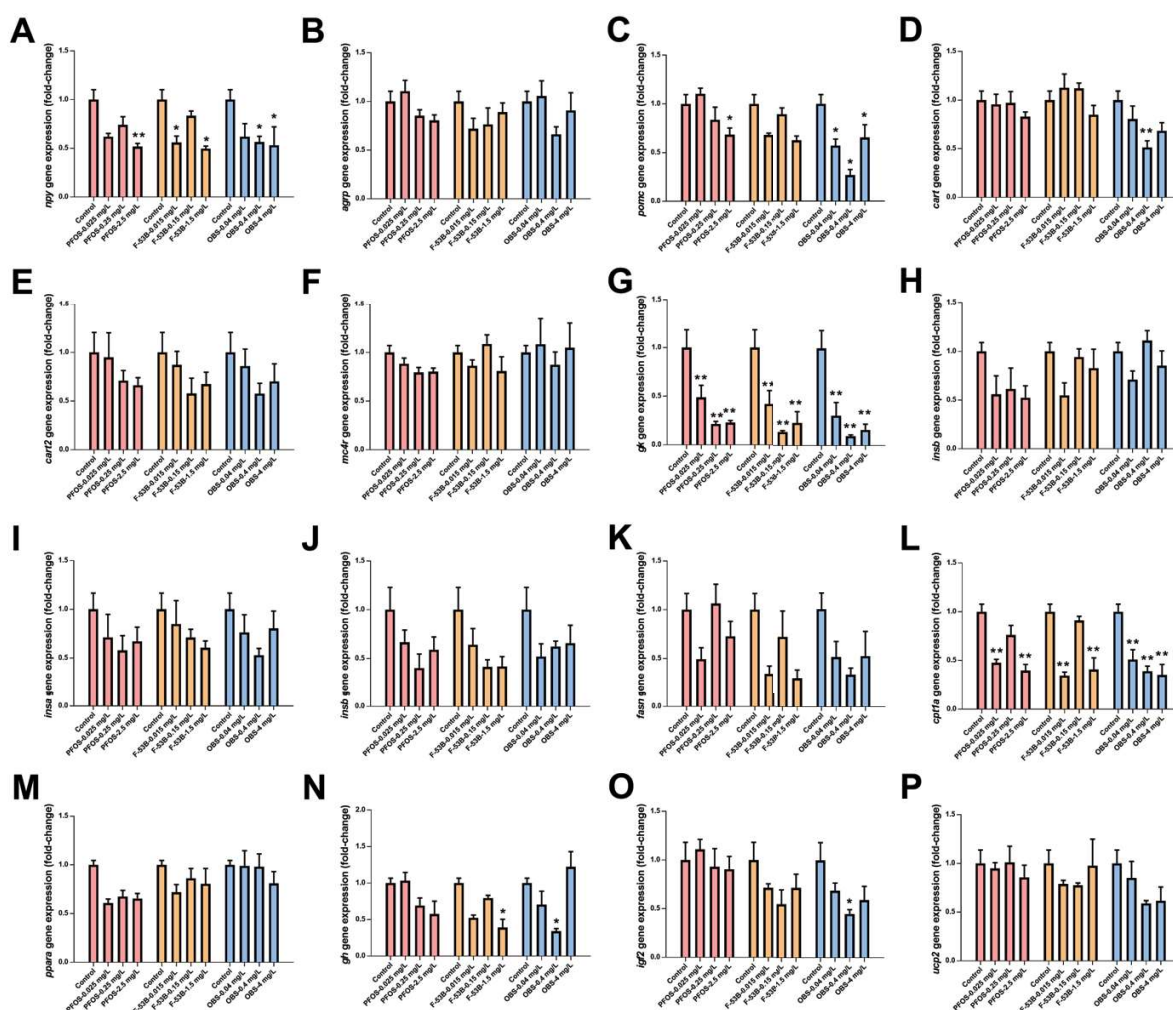
721 **Figure 3**



722

723

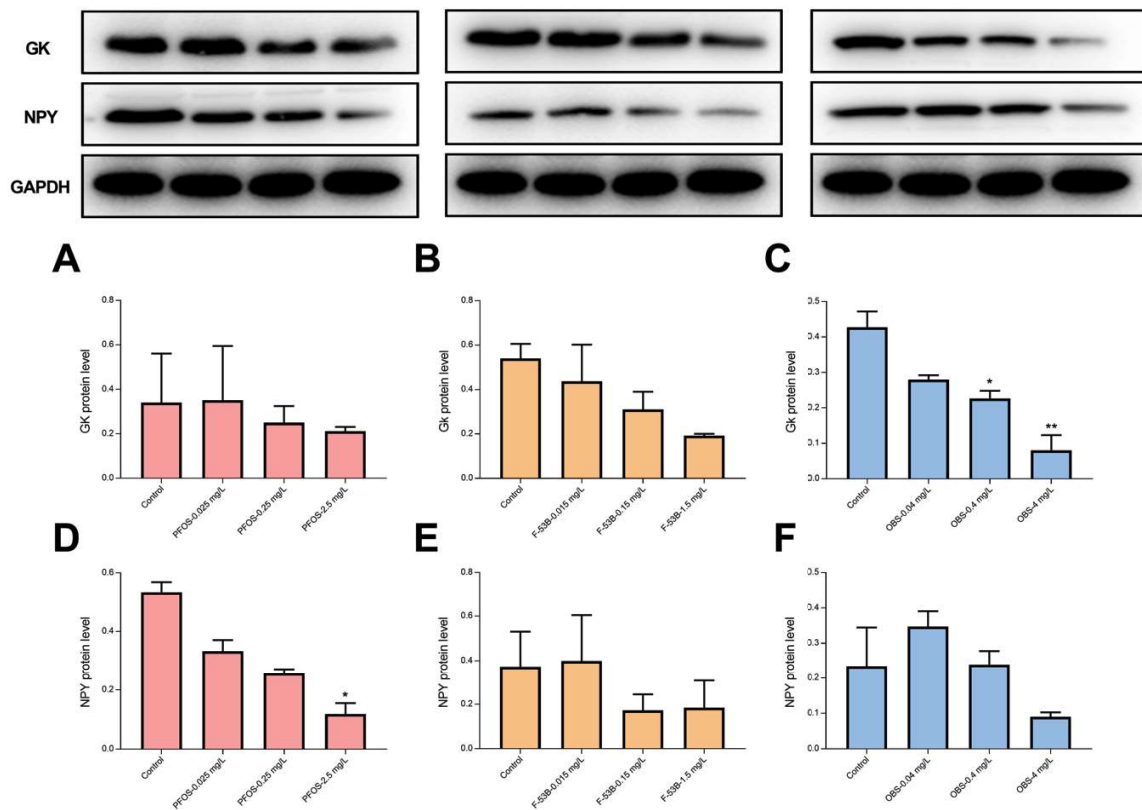
724 **Figure 4**



725

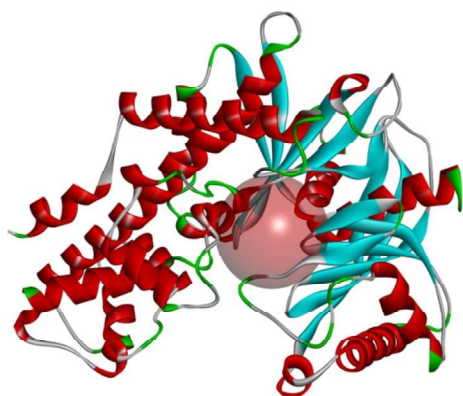
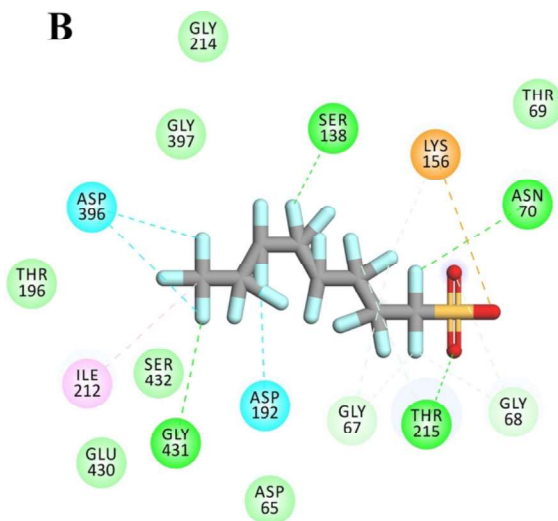
726

727 **Figure 5**

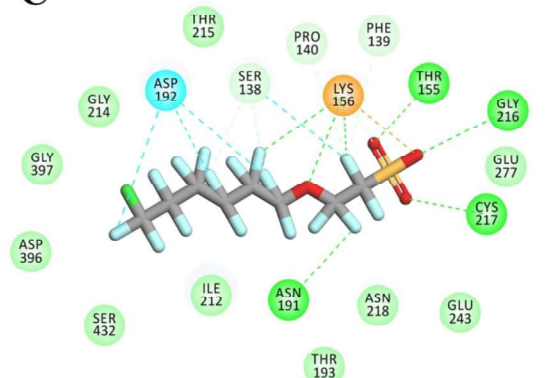


728

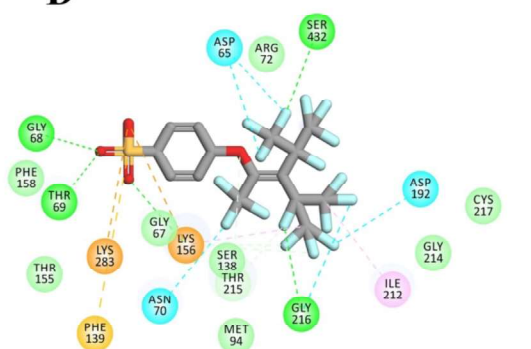
729

730 **Figure 6****A****B****Interactions**

van der Waals	Carbon Hydrogen Bond
Attractive Charge	Halogen (Fluorine)
Conventional Hydrogen Bond	Alkyl

**C****Interactions**

van der Waals	Carbon Hydrogen Bond
Salt Bridge	Halogen (Fluorine)
Conventional Hydrogen Bond	

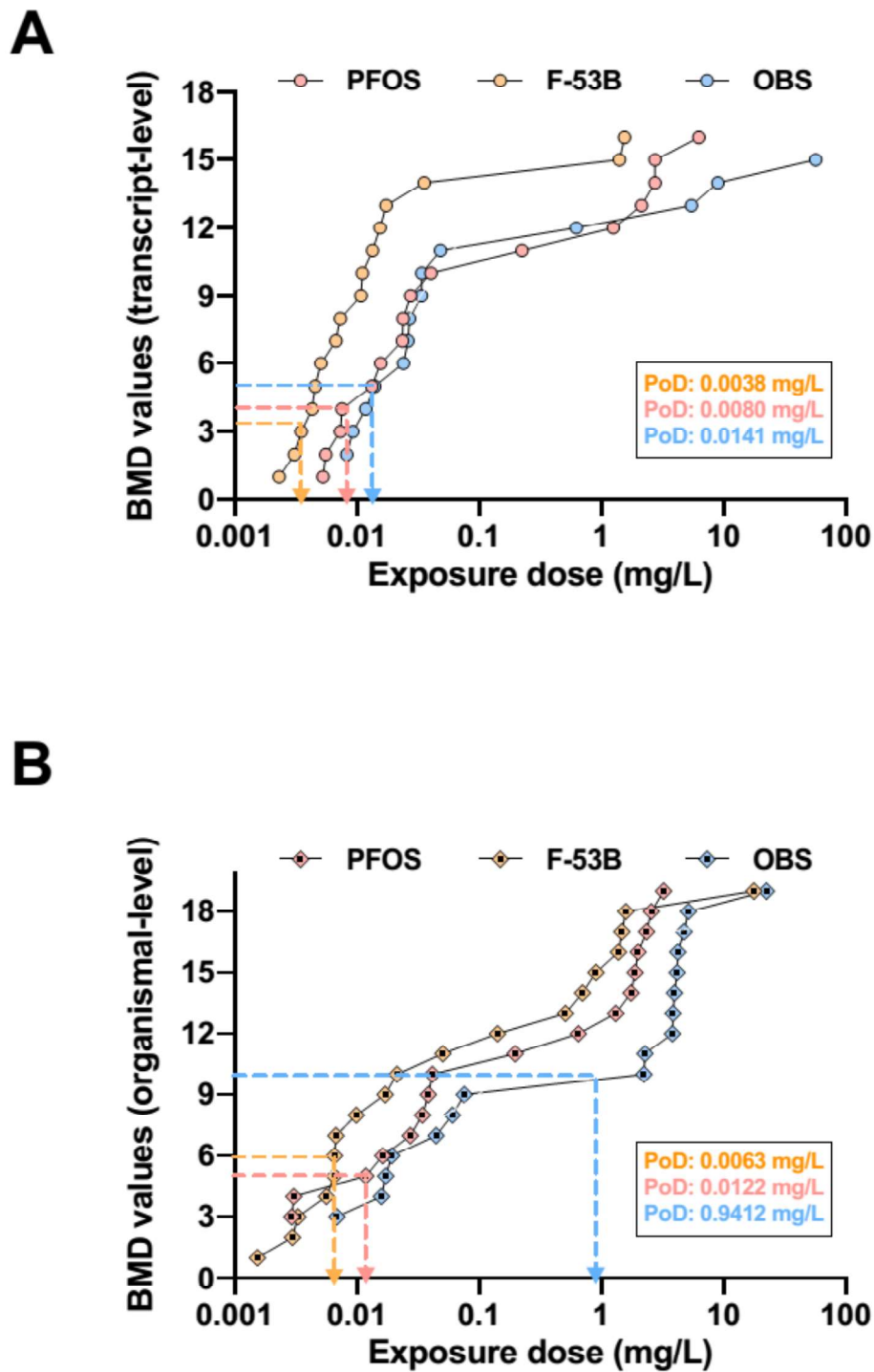
**D****Interactions**

van der Waals	Halogen (Fluorine)
Attractive Charge	Pi-Sulfur
Conventional Hydrogen Bond	Alkyl
Carbon Hydrogen Bond	

731

732

733 Figure 7



734